



Open Archive TOULOUSE Archive Ouverte (OATAO)

OATAO is an open access repository that collects the work of Toulouse researchers and makes it freely available over the web where possible.

This is an author-deposited version published in : <http://oatao.univ-toulouse.fr/>
Eprints ID : 19415

To link to this article : DOI: 10.1016/j.electacta.2017.01.160
URL : <http://dx.doi.org/10.1016/j.electacta.2017.01.160>

To cite this version : Lan, Yandi and Coetsier, Clémence and Causserand, Christel and Serrano, Karine *On the role of salts for the treatment of wastewaters containing pharmaceuticals by electrochemical oxidation using a boron doped diamond anode.* (2017) *Electrochimica Acta*, vol. 231. pp. 309-318. ISSN 0013-4686

Any correspondence concerning this service should be sent to the repository administrator: staff-oatao@listes-diff.inp-toulouse.fr

On the role of salts for the treatment of wastewaters containing pharmaceuticals by electrochemical oxidation using a boron doped diamond anode

Yandi Lan, Clémence Coetsier, Christel Causserand, Karine Groenen Serrano*

Laboratoire de Génie Chimique, CNRS, INPT, UPS Université de Toulouse, 118 route de Narbonne, F-31062 Toulouse, France

ARTICLE INFO

ABSTRACT

Refractory pharmaceuticals remain in biologically treated wastewater and are continuously discharged into aquatic systems due to their limited biodegradability. Electrochemical oxidation is promising for the treatment of such refractory compounds, in particular using a boron doped diamond (BDD) anode. This study investigates the role of salts, such as sulfates and chlorides in the electrochemical treatment of wastewater. The presence of sulfates accelerated the removal of ciprofloxacin and sulfamethoxazole, but had no effect on the oxidation of salbutamol. This comparison highlights the selectivity of the reaction between organics and sulfate radicals. The addition of chlorides into the solution led to a remarkably-faster degradation of ciprofloxacin. However, incomplete mineralization was observed at high current densities due to the significant formation of halogenated organic compounds (AOX). The formation of refractory and toxic compounds such as ClO_4^- and AOX can be limited under the control of (i) applied current intensity and (ii) duration of electrolysis. Electrochemical oxidation of concentrated biologically-treated hospital wastewater investigated the excellent removal of biorefractory pharmaceuticals and confirmed the acceleration effect of salts on pharmaceutical degradation.

1. Introduction

Recently, numerous studies have demonstrated the occurrence of micropollutants, especially biorefractory pharmaceuticals, in the aquatic environment [1–4]. They pose significant threats to the sustainability of both ecosystems and the safety of drinking water [5,6]. These molecules seem to be neither fully eliminated in the conventional wastewater treatment plant with activated sludge treatment [7–9] nor using a membrane bioreactor (MBR) process [10]. Consequently, an alternative technique is required for their efficient elimination at source before disposal and dilution in sewerage system.

It is well known that electrochemical oxidation using a BDD anode represents a promising technique for the elimination of persistent organics [11]. Indeed, the strong oxidation ability of the BDD anode is due to the electrogeneration of hydroxyl radical ($\cdot\text{OH}$) from the water discharge (Eq. 1).



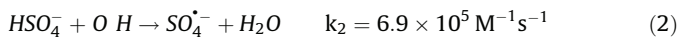
It is commonly assumed that electrogenerated hydroxyl radicals, the most powerful oxidants in water (standard potential $E^\circ = 2.74 \text{ V} / \text{SHE}$ [12]), are very active in the degradation of organic molecules via the transfer of oxygen atoms. Numerous studies were carried out to investigate the electrochemical behavior of the BDD anode for the removal of pharmaceutical products, such as 17 β -estradiol [13], estrone [14], paracetamol [15], sulfamethoxazole [16,17], atenolol [18] and trimethoprim [17] in synthetic solutions. In all cases, total mineralization has been achieved. Moreover, coupling processes using a step to preconcentrate the micropollutants, followed by the electro-oxidation with the BDD anode were performed for the treatment of real wastewater. Urriaga's group carried out a pilot system that integrated ultrafiltration (UF), reverse osmosis (RO) and electrochemical oxidation (EO) of effluents from wastewater treatment plants [19,20]. A group of 12 pharmaceutical products was selected to monitor their degradation by the coupling processes. The treatment of the solution by RO and EO coupling significantly reduced the total micropollutants. A previous study in our group performed the electrochemical oxidation coupling with nanofiltration (NF) for the treatment of biologically-treated hospital wastewater (by membrane bioreactor treatment) [21]. The results demonstrated that rapid mineralization occurred: the removal of total organic carbon

* Corresponding author.

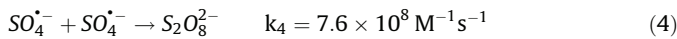
E-mail address: serrano@chimie.ups-tlse.fr (K. Groenen Serrano).

(TOC) and chemical oxygen demand (COD) reached 97% and 100%, respectively. Moreover, it was noticed that the COD of NF retentate decayed at a faster rate than the theoretical values and the experimental values obtained in a synthetic solution at the end of electrolysis. It can be assumed that a distinct oxidation phenomenon proceeds in addition to EO. With a BDD anode, it is possible to generate strong oxidants from salts such as sulfates, carbonates, and chlorides which are present in the solution [22]. These oxidants can act as indirect oxidants for the mineralization of micropollutants near the anode and/or in the bulk of the solution.

More specifically, sulfate ions which are often present in both liquid effluents and in natural water can be considered to be an active electrolyte. Strong oxidants such as sulfate radicals ($SO_4^{\bullet-}$) and persulfate ($S_2O_8^{2-}$) can be electrogenerated using a BDD anode [23]. The mechanism of the formation of sulfate radicals and persulfate is well known; only HSO_4^- and undissociated H_2SO_4 react with $\bullet OH$ radicals to form sulfate radicals [24].



The radical $SO_4^{\bullet-}$ may produce $S_2O_8^{2-}$ by recombination [24].

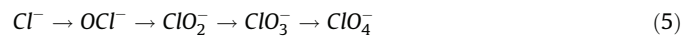


Recent studies have reported the influence of the presence of sulfate on the removal of pharmaceuticals. Muruganathan et al. have observed that the effective mineralization of ketoprofen can only be achieved when the supporting electrolyte was Na_2SO_4 , comparing to $NaNO_3$, $NaCl$ and explained this phenomenon to the generation of $S_2O_8^{2-}$ and $SO_4^{\bullet-}$ from SO_4^{2-} with a BDD anode [25]. However, the actual role of sulfate and the relative electro-generated oxidants in degradation of pharmaceutical products is not sufficient clear. Therefore, further studies are needed to investigate the role of these oxidants in the degradation of pharmaceuticals.

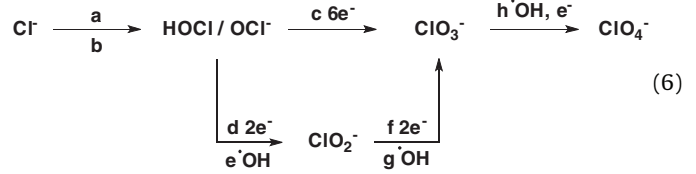
The presence of chloride ions allows increasing the efficiency of the degradation of organics, while at the same time, toxic perchlorate and halogenated organic compounds can be formed during the treatment using BDD anode [26–30]. Since these compounds pose a serious hazard for drinking water and aquatic ecosystems [31,32] and are resistant to further oxidation, it is extremely important to minimize the formation of these compounds during water treatment.

Previous works have investigated that ClO_4^- is generated via a multistep oxidation pathway from chloride, as shown in reaction

(5) [32].



Using a BDD anode, besides direct electron transfer reactions, the electro-oxidation pathway of Cl^- also includes the chemical oxidation reactions with hydroxyl radicals [33–39]. The possible pathway is exhibited in reaction scheme (6) listed in Table 1.



Moreover, reactions of addition and substitution between the organics and the active chlorine species (e.g. Cl_2 , OCl^- , $HOCl$) or chlorine radicals (Cl^\bullet , $Cl_2^{\bullet-}$) are mainly responsible for the formation of undesired halogenated organic compounds [32].

Few studies discuss about possibility to control the production of perchlorate and halogenated organic compounds using BDD anode during the electrooxidation process. Bergmann et al. has indicated that a lower current density and a higher flow rate may reduce perchlorate production, but these actions also led to a decrease in the treatment efficiency [26]. Donaghue and Chaplin have investigated that the presence of organics in the solution inhibits the formation of ClO_4^- [43]. This was mainly due to the fact that organics react with higher $\bullet OH$ reaction rates than the reaction between ClO_3^\bullet and $\bullet OH$ to form ClO_4^- (reaction h, Table 1). Costa et al. have found that the formation of halogenated organic compounds is favored in an acidic pH [27]. Schmalz et al. have demonstrated that the formation of halogenated organic compounds correlated with the electrical charge and didn't depend on the current density under their experimental conditions during electrochemical disinfection of biologically-treated wastewater [28].

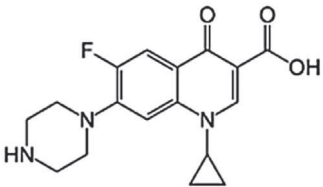
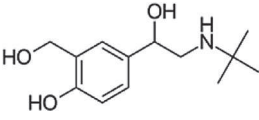
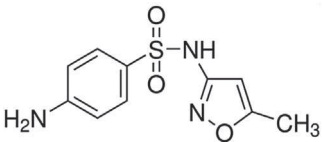
Considering the presence of various salts in real wastewater and the uncommon electrochemical properties of the BDD anode allowing the possible formation of perchlorate and halogenated organic compounds, a specific study is needed to suggest the appropriate operating conditions to limit the formation of undesired and toxic species.

The object of the present study is to investigate the positive and negative impacts of the presence of salts (chloride, sulfate, carbonate anions and calcium, magnesium cations) in the electrochemical treatment of wastewaters containing

Table 1
Reactions of chlorine species during electrolysis.

	Reaction		Ref.
a	$Cl^- \rightarrow BDD(Cl^\bullet) + e^-$ $Cl^\bullet + Cl^\bullet \rightarrow Cl_2$	$E^0 = 1.36V$	[40,41]
b	$Cl_2 + H_2O \rightarrow HOCl + Cl^- + H_2O$ $Cl^- + {}^{null}OH \leftrightarrow ClOH^-$		
c	$6HOCl^- + 3H_2O \rightarrow 2ClO_3^- + 4Cl^- + 12H^+ + 3/2O_2 + 6e^-$ $6OCl^- + 3H_2O \rightarrow 2ClO_3^- + 4Cl^- + 6H^+ + 3/2O_2 + 6e^-$	$k = 4.3 \times 10^9 M^{-1} s^{-1}$ $E^0 = 0.46V$	[42] [33]
d	$OCl^- + 2OH^- \rightarrow ClO_2^- + H_2O + 2e^-$	(alkaline solution)	[35]
e	$\bullet OH + OCl^- \rightarrow \bullet ClO + OH^-$ $\bullet OH + \bullet OCl^- \rightarrow ClO_2 + H^+$	$k = 9 \times 10^9 M^{-1} s^{-1}$ $k > 1 \times 10^9 M^{-1} s^{-1}$	[34]
f	$ClO_2^- + 2OH^- \rightarrow ClO_3^- + H_2O + 2e^-$	(alkaline solution)	[35]
g	$\bullet OH + ClO_2^- \rightarrow \bullet ClO_2 + OH^-$ $\bullet OH + \bullet ClO_2 \rightarrow ClO_3^- + H^+$	$k = 6 \times 10^9 M^{-1} s^{-1}$ $k = 4 \times 10^9 M^{-1} s^{-1}$	[34]
h	$\bullet ClO_3 + \bullet OH \rightarrow HClO_4$		[39]

Table 2
Structure of target pharmaceuticals.

	Ciprofloxacin (CIP)	Salbutamol (SALBU)	Sulfamethoxazole (SMX)
Formula	C ₁₇ H ₁₈ FN ₃ O ₃	C ₁₃ H ₂₁ NO ₃	C ₁₀ H ₁₁ N ₃ O ₃ S
Molecular weight (g mol ⁻¹)	331.3	239.3	253.3
Structure			

pharmaceuticals. This is the aim of proposing adequate operating conditions to limit the risk of formation of toxic by-products. For that, a first section performed in synthetic solutions is devoted to the study of the interaction between salts, such as chlorides and sulfates with hydroxyl radicals generated at the anode surface under anodic polarization. The consequences on the removal on three targeted pharmaceuticals: ciprofloxacin, salbutamol and sulfamethoxazole are studied. Particular attention has been paid on the conversion and variation in concentrations of chlorine species, as well as the formation of halogenated organic compounds. Based on these studies in synthetic solutions, electrochemical oxidation treatment of nanofiltration retentate of biologically-treated hospital wastewater was performed. In view to the application of the process in real wastewater, it is studied the effect of the composition of the real matrix on (i) the performance of the mineralization of pharmaceutical products, (ii) the formation of by-products and (iii) the scaling on the cathode.

2. Material and methods

2.1. Chemicals and solutions

2.1.1. Chemicals

The ciprofloxacin (CIP) ($\geq 98\%$ purity) was purchased from Fluka Company. USA). The salbutamol (SALBU) (Salbutamol-sulfate $\geq 99\%$ purity) and sulfamethoxazole (SMX) ($\geq 98\%$ purity) were obtained from Alfa Aesar and Fluka, respectively. All synthetic solutions were prepared with ultrapure water ($\rho = 18.2 \text{ M}\Omega \text{ cm}$). The structures of these molecules are reported in Table 2. Potassium sulfate ($\geq 99\%$ purity) and potassium chloride ($\geq 99\%$ purity) were analytical grade and supplied by Fisher Science. Other chemicals, organics or solvents were HPLC or analytical grade.

2.1.2. Wastewater source

The hospital wastewater was treated by a membrane bioreactor (MBR) installed at Purpan hospital located in Toulouse, France [44]. It was directly fed from the hospital's sanitary collection system. MBR effluent contains salts, organics (total organic carbon around 20 mg L^{-1}) and around 50 pharmaceuticals from 10 different therapeutic classes [44]. Before electrochemical treatment, the MBR effluent was firstly concentrated by a NF process [21].

The batch filtration was conducted in a cross-flow filtration unit. The polyamide membrane: NE70 was installed into a stainless cross-flow cell (Sepa CF II, Osmonics) in which the effective membrane area was $1.4 \times 10^{-2} \text{ m}^2$. The NF retentate was collected for a volume reduction factor of 5 (VRF=5, correlating to the 80% recovery) which is within the range that would be applied in a full-scale system (30 - 90%). The NF retentate was the mixture from

several filtrations. The characteristics of the wastewater matrix (NF retentate of MBR effluents) are presented in Table 3.

2.2. Analytical techniques

Concentrations of salts in synthetic solution and wastewater were measured by ionic chromatography with an ICS 3000 system (Dionex, France). The injection volume was $25 \mu\text{L}$ and the column temperature was set at 30°C . The concentrations of anions and cations were analyzed with two columns (Thermo Scientific, Dionex): IonPacTM AS11 (mobile phase: 95% of 5 mM NaOH and 5% of 100 mM NaOH), IonPacTM CS12 (mobile phase: $\text{CH}_4\text{O}_3\text{S}$ 20 mM), respectively. Analytical errors for anions and cations ranged from 1.5% (Cl^-) to 6% (SO_4^{2-}). In this mobile phase, HClO was reported as ClO^- .

Pharmaceutical concentrations were measured by high performance liquid chromatography connected with an ultraviolet-visible spectrometry detector (HPLC-UV). The analyses were conducted on Agilent 1200 Series HPLC systems (Agilent Technologies, USA). An Agilent ZORBAX Eclipse Plus C18 column ($3.5 \mu\text{m}$, $3 \text{ mm} \times 100 \text{ mm}$) from Agilent Technologies was used. The detection UV wavelength was set to 278 nm. The mobile phase of HPLC consisted of a gradient of ultrapure water (with 0.1% formic acid) and acetonitrile (with 0.1% formic acid) and the column temperature was set to 30°C . The flow rate was 0.4 mL min^{-1} and the volume of injection was $10 \mu\text{L}$. The detection limit of ciprofloxacin and sulfamethoxazole is $10 \mu\text{g L}^{-1}$ and $100 \mu\text{g L}^{-1}$ for Salbutamol. The analytical errors range from 0.2% to 1%.

Adsorbable organic halogens (AOXs) were analyzed in accordance with the ISO 9562 Method [45]. ISO 9562 usually specifies the methodology for the direct determination of a concentration of $10 \mu\text{g L}^{-1}$ in water for organochlorine, bromine and iodine (expressed as chloride) adsorbable on activated carbon.

TOC and inorganic carbon (HCO_3^- in experimental conditions) were measured with a TOC-VCSN instrument (Shimadzu). The concentration of inorganic carbon was measured after acidification

Table 3
Physico-chemical characteristics and composition of the wastewater after NF.

Properties and target pharmaceutical	Value	Ions	Concentration (mg L ⁻¹)
pH	7.84	Na ⁺	161
Conductivity (mS cm ⁻¹)	1.2	K ⁺	34
COD (mg L ⁻¹)	86	Mg ²⁺	9
TOC (mg L ⁻¹)	40	Ca ²⁺	70
UV ₂₅₄	1.13	Cl ⁻	70
AOX ($\mu\text{g Cl L}^{-1}$)	2300	NO ₃ ⁻	152
		SO ₄ ²⁻	110
Target pharmaceutical	PO ₄ ³⁻	13	
Ciprofloxacin ($\mu\text{g L}^{-1}$)	81	HCO ₃ ⁻	63

and degassing, performed automatically. TOC was calculated from the difference between the total carbon and inorganic carbon. COD was determined by photometry using disposable test tubes (HI93754H-25 LR from HANNA Instruments) and a HACH DR/2400 photometer. Test tubes were heated at 150 °C for 2 hours and left to cool down at room temperature before measurement. The analytic errors for TOC and COD were estimated to 5%.

2.3. Electrochemical set-up

The experimental solution was stored in a thermoregulated glass reservoir (1) and circulated through the electrochemical cell using a centrifugal pump (2) (Fig. 1). The flow rate was 360 L h⁻¹ and the volume of the solution was 1L. Electrolyses were conducted at 30 °C in a one-compartment flow filterpress reactor under galvanostatic conditions (3). Electrodes were two discs of 69 cm² of active surface. The BDD anode from Waterdiam (Switzerland) was elaborated by chemical vapor deposition on a conductive substrate of silicium. The cathode was a 1 mm thick disc of zirconium. The current was supplied by an ELCAL 924 power supply. The mass transfer coefficient can be determined by Eq. 7 in the operating range of flow rate (120 - 300 L h⁻¹) at 30 °C [46]:

$$k_d \times 10^5 = 0.0051\Phi + 0.4367 \quad (7)$$

where, k_d is the mass transfer coefficient (m s⁻¹), Φ is the flow rate in L h⁻¹

In the present study, the mass transfer coefficient corresponding to the flow rate of 360 L h⁻¹ equals 2.30 × 10⁻⁵ m s⁻¹. Before each electrolysis, the working electrodes were anodically pretreated (40 mA cm⁻² for 30 min in a 0.1 M K₂SO₄ solution) to clean their surfaces of any possible adsorbed impurities. Then the system was rinsed by ultrapure water. Samples were taken at regular intervals in the tank. The global volume of samples was less than 10% of the total volume.

According to the properties of the BDD anode, limiting current density can be defined by using a global parameter, the COD [47].

$$i_{lim} = 4Fk_dCOD \quad (8)$$

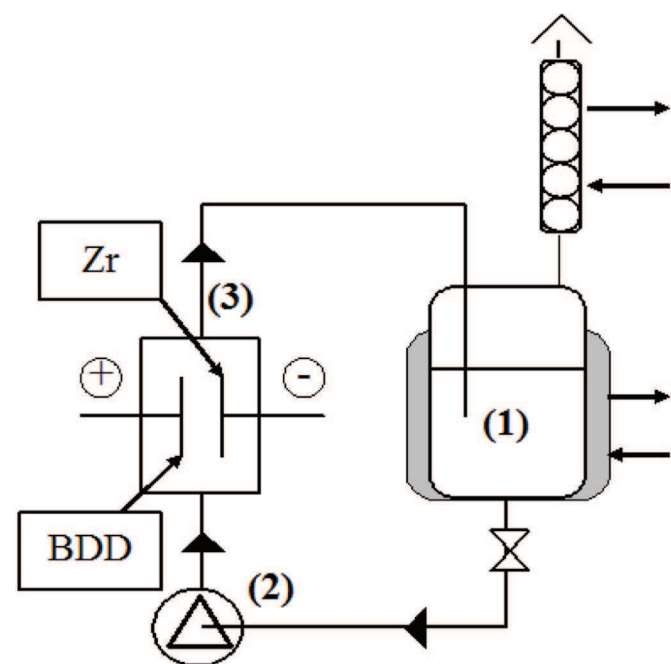


Fig. 1. Discontinuous process with a single compartment electrochemical reactor, (1) a tank, (2) a pump, and (3) an electrochemical cell.

where i_{lim} is the limiting current density for the mineralization of organics (A m⁻²), F is the Faraday constant (C mol⁻¹) and COD is in molO₂ m⁻³.

Depending on the value of the current density (i), two different kinetic regimes can be defined: (1) $i < i_{lim}$: the kinetics of the reaction is charge controlled; (2) $i > i_{lim}$: the kinetics of the reaction is controlled by mass transfer. In this paper, the oxidation was under mass transfer control ($i > i_{lim}$), thus the evolution of COD with time can be expressed as equation (9):

$$COD(t) = COD^0 \exp\left(-\frac{Ak_d t}{V}\right) \quad (9)$$

where V and A are the volume of the solution (m³) and the electrode surface (m²), respectively.

In all electrolyses presented in this paper, the oxidation was under mass transfer control and for [CIP]₀ = 0.0695 mM, the corresponding i_{lim} = 1.29 mA.

3. Results and discussion

3.1. Electrochemical oxidation of pharmaceuticals

Fig. 2 shows the decay of pharmaceuticals (ciprofloxacin, salbutamol or sulfamethoxazole) during the electrolysis. The complete removal of these pharmaceuticals is observed at around 250 min.

The comparison of the three pharmaceuticals shows an exponential decay according to the process limited by mass transfer ($i > i_{lim}$) (Eq. 8). The removal of pharmaceuticals follows a pseudo first-order reaction (Eq. 10). The kinetic analysis is shown in the inset panel of Fig. 2.

$$\ln\frac{C_t}{C_0} = -k_{obs}t \quad (10)$$

where t is the electrooxidation time; C_0 and C_t are the initial concentration of pharmaceutical compound and concentration at time t , respectively; k_{obs} is the observed degradation rate of pharmaceuticals.

The degradation rate of the three pharmaceuticals are almost the same (0.0203 min⁻¹, 0.0208 and 0.0168 min⁻¹, for CIP, SALBU and SMX, respectively) with a slight difference with SALBU.

It is well known that electrogenerated hydroxyl radicals react massively with organics without selectivity. These reactions occur very close to the BDD anode. The main pathways of •OH reactions

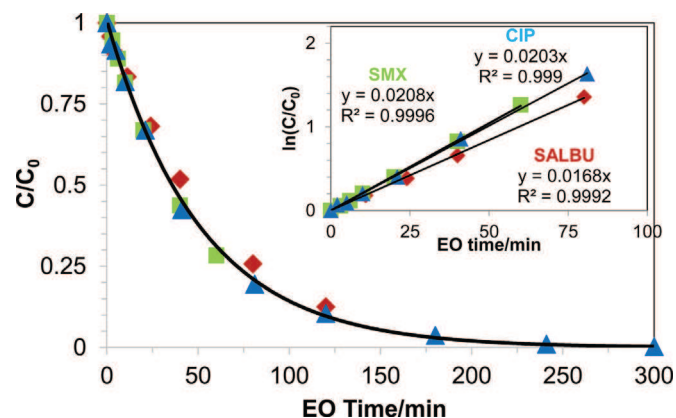


Fig. 2. Concentration variation of ▲ ciprofloxacin (CIP), ◆ salbutamol (SALBU), ■ sulfamethoxazole (SMX) during electrolysis in 1L of K₂SO₄ 0.02 mol L⁻¹. Operating conditions: [SALBU]₀ = 0.0671 mmol L⁻¹, i = 7.25 mA cm⁻²; [SMX]₀ = 0.0596 mmol L⁻¹, i = 7.25 mA cm⁻²; [CIP]₀ = 0.0695 mmol L⁻¹, i = 1.45 mA cm⁻². Inset panel: kinetic analysis of pharmaceuticals of SALBU, SMX and CIP during EO.

with pharmaceuticals are additions to C-C, C-N and C-S double bonds and H-abstraction [33]. The kinetics of most addition reactions are very high, typically in the order of 10^9 - $10^{10} \text{ M}^{-1} \text{ s}^{-1}$ [48,49]. Consequently, the degradation of pharmaceuticals under mass transfer control is not selective and mainly depends on the mass transfer coefficient.

3.2. Effect of sulfate ions on pharmaceuticals elimination

As mentioned previously, only HSO_4^- and undissociated H_2SO_4 react with $\cdot\text{OH}$ radicals to form $\text{SO}_4^{\bullet-}$ and $\text{S}_2\text{O}_8^{2-}$ (Eq. 2-4). To investigate the role of sulfate species on the removal of pharmaceuticals, the results obtained in Fig. 2 were compared with the ones obtained in K_2SO_4 0.1 M (pH=3.7 adjusted with H_2SO_4 0.1 M solution). In K_2SO_4 solutions, sulfate anions, hydrogenosulfate anions and undissociated sulfuric acid coexist, depending on the pH. The concentration of each species can be calculated from the dissociation constants of Eq. 11 and 12 [50].

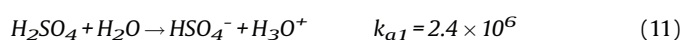


Table 4 presents the concentrations of HSO_4^- and SO_4^{2-} and the pharmaceuticals in both solutions. The main form of sulfate is SO_4^{2-} , the concentration of undissociated H_2SO_4 is negligible. Moreover, it can be observed that the concentration of HSO_4^- in a K_2SO_4 0.02 M solution is 2000 times lower than in a K_2SO_4 0.1 M pH = 3.7. Consequently, the production of $\text{SO}_4^{\bullet-}$ and $\text{S}_2\text{O}_8^{2-}$ is less significant in K_2SO_4 0.02 M solution.

Fig. 3 shows the degradation of SALBU, SMX and CIP in both electrolytes. It is interesting to observe that the effect of electrolyte composition depends on the nature of the pharmaceuticals.

The same degradation rate of SALBU was observed (Fig. 3 (a)) in both electrolytes whatever the conductivity of the solution (4.7 mS cm^{-1} for $[\text{K}_2\text{SO}_4] = 0.02 \text{ M}$ and 20 mS cm^{-1} for $[\text{K}_2\text{SO}_4] = 0.1 \text{ M}$). However, greater degradation rates of SMX (Fig. 3 (b)) and CIP (Fig. 3 (c)) were obtained in K_2SO_4 0.1 M, which indicates that another phenomenon occurred in both electrolyses. Additional chemical reactions between organics and electrogenerated oxidants from hydrogenosulfate anions, such as sulfate radicals or persulfate anions (Eq. 3 and 4) can explain these results. Thermodynamically, $\text{SO}_4^{\bullet-}$ ($E^\circ = 2.6 \text{ V}$) is a stronger oxidant than $\text{S}_2\text{O}_8^{2-}$ ($E^\circ = 2.01 \text{ V}$). $\text{SO}_4^{\bullet-}$ can react selectively and rapidly with pharmaceuticals that are close to the anode surface, with an order of 10^9 - $10^{10} \text{ M}^{-1} \text{ s}^{-1}$ [51], while the reaction of $\text{S}_2\text{O}_8^{2-}$ with many organics is kinetically slow [52]. Moreover, it was reported that $\text{S}_2\text{O}_8^{2-}$ was not capable of oxidizing CIP and SMX without activation to $\text{SO}_4^{\bullet-}$ [53]. Therefore, the $\text{SO}_4^{\bullet-}$ plays a dominant role on the additional oxidation of pharmaceuticals in the presence of hydrogenosulfate.

In general, $\text{SO}_4^{\bullet-}$ is more likely to participate in electron transfer reactions [49,51,54] than $\cdot\text{OH}$ which is more likely to participate in hydrogen abstraction or addition reactions [55,56]. The former reactions are selective while the later ones are non-

Table 4

Concentration of SO_4^{2-} , HSO_4^- and pharmaceuticals in synthetic solutions at initial time.

Concentration (mol L^{-1})	$[\text{K}_2\text{SO}_4] = 0.1 \text{ mol L}^{-1}$ pH = 3.7	$[\text{K}_2\text{SO}_4] = 0.02 \text{ mol L}^{-1}$ pH = 6.4 (initial)
$[\text{SO}_4^{2-}]$	9.8×10^{-2}	2×10^{-2}
$[\text{HSO}_4^-]$	1.9×10^{-3}	8×10^{-7}
[SALBU]	6.77×10^{-5}	6.71×10^{-5}
[SMX]	6.23×10^{-5}	6.95×10^{-5}
[CIP]	6.23×10^{-5}	6.95×10^{-5}

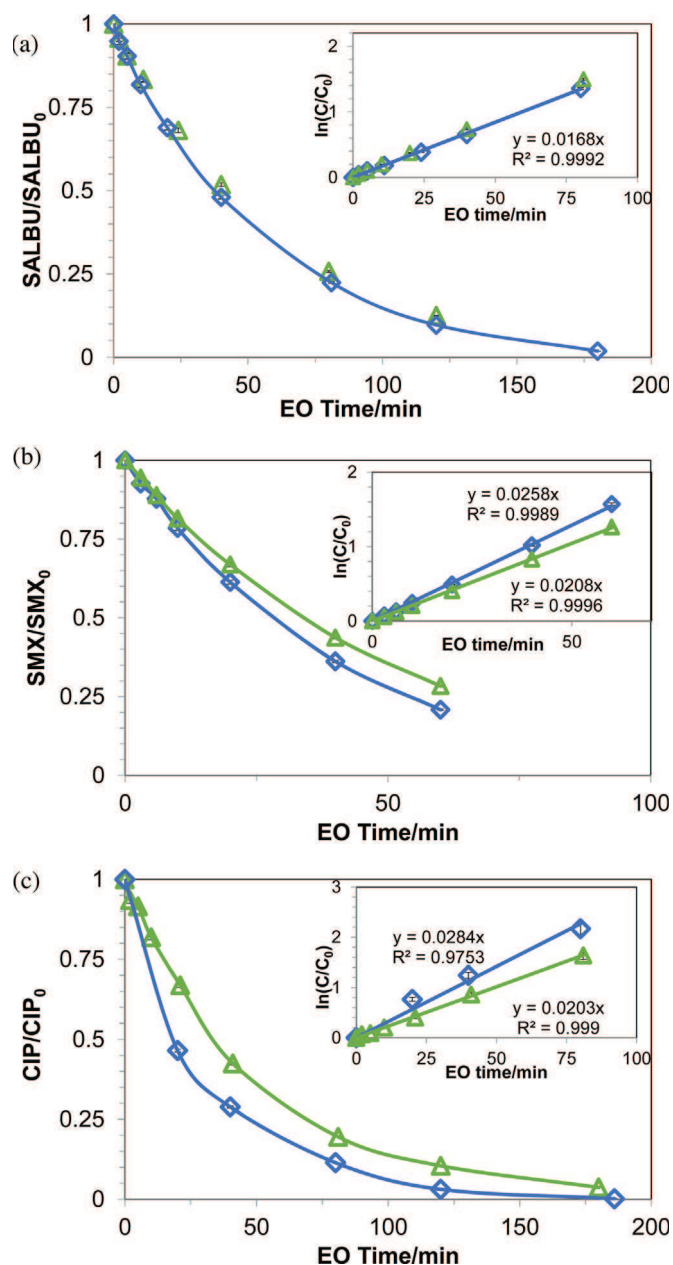


Fig. 3. The normalized concentration of pharmaceuticals during electrolyses: (a) SALBU, $i = 7.25 \text{ mA cm}^{-2}$; (b) SMX, $i = 7.25 \text{ mA cm}^{-2}$; (c) CIP, $i = 1.45 \text{ mA cm}^{-2}$ in \diamond K_2SO_4 0.1 mol L^{-1} , pH = 3.7; \triangle K_2SO_4 0.02 mol L^{-1} , pH range = 6.4-4; $i > i_{\text{lim}}$. Error bars = 1%. Inset panel: kinetic analysis of pharmaceuticals during EO.

selective. The acceleration phenomena were observed in the degradation of SMX and CIP but not in SALBU, which exclusively correlates with the fact that $\text{SO}_4^{\bullet-}$ reacts selectively with organics.

Overall, the electrogenerated $\text{SO}_4^{\bullet-}$ also accelerated the removal of TOC (Fig. 4) and COD (not shown). Results show that 84% of TOC and 100% of COD was removed in a K_2SO_4 0.1 M solution, while in a K_2SO_4 0.02 M solution, only 71% of TOC and 86% of COD was removed after 300 min of electrolysis.

3.3. Electrochemical oxidation of pharmaceuticals in the presence of chloride

To investigate the role of Cl^- during electrolysis, besides the pharmaceutical degradation, it is important to study the conversion of chlorine species and the formation of AOXs, which could be

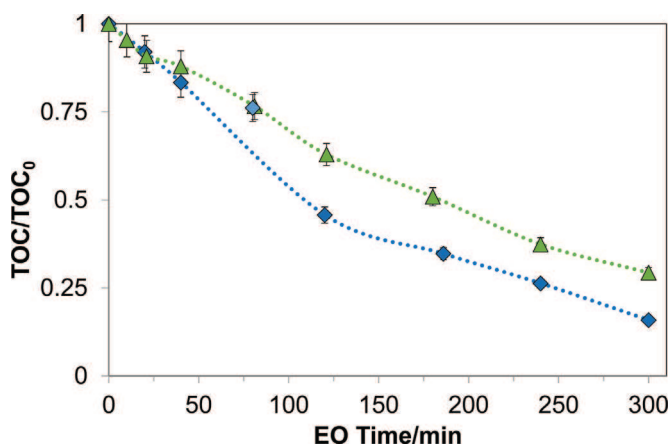


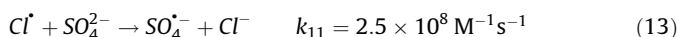
Fig. 4. Normalized variation of TOC during electrolysis of 1L of CIP solution. \blacklozenge K_2SO_4 0.1 mol L^{-1} , initial pH=4, $[\text{TOC}]_0 = 10.4 \text{ mg L}^{-1}$, \blacktriangle K_2SO_4 0.02 mol L^{-1} , initial pH=6.4, $[\text{TOC}]_0 = 11.2 \text{ mg L}^{-1}$; $i^0_{\text{lim}} = 1.45 \text{ mA cm}^{-2}$ ($i > i^0_{\text{lim}}$), error bars=5%.

a potential environmental hazard. The range of the Cl^- concentration in a synthetic solution was chosen according to the concentration range in the NF retentate (Table 3).

3.3.1. Oxidation of CIP and Cl^-

Fig. 5 (a) shows the degradation of CIP in the presence and absence of chlorides for the specific applied current densities close to the limiting current density.

The obvious acceleration for CIP degradation is observed in the presence of Cl^- : the complete removal of CIP was reached at 80 min in the presence of Cl^- while 240 min in absence of Cl^- . Moreover, the presence of Cl^- also posed a significant positive effect on the removal of TOC (Fig. 5 (b)). After an electrolysis time of 300 min, 90% of TOC removal was reached, compared to only 70% without Cl^- ions. The acceleration effect of the presence of chloride ions in this study correlated with the electrogenerated active chlorine (Cl_2 , HClO or ClO^-) which can indirectly oxidize the organics [13,14,57,58]. Moreover, due to the electrochemical properties of BDD, chloride radical (Cl^*) is the first-step product of direct oxidation of chloride with BDD anode [40] (Table 1, reaction a). Besides active chlorine, additional inorganic oxidants such as $\text{SO}_4^{\bullet-}$ can be formed from the reaction between Cl^* and SO_4^{2-} [59] (Eq.13). This radical also play a positive role in the oxidation of organics.



The effect of the presence of Cl^- on mineralization of pharmaceuticals seems to be surprisingly adverse at a high applied current density. It has been found that TOC removal reached 90% in the presence of Cl^- at 1.45 mA cm^{-2} ($i \approx i^0_{\text{lim}}$), while decreased dramatically to 40% at 43.5 mA cm^{-2} ($\frac{i}{i^0_{\text{lim}}} > 30$). The efficiency of mineralization highly related to the applied current density. Low removal of TOC may be attributed to the possible formation of halogenated organic compounds during electrolysis. To explain this surprising effect, a further study in the next section focuses on the formation of halogenated organic compounds and the conversion of chlorine species.

3.3.2. Conversion of chloride and formation of AOXs

To understand the conversion of chloride during electrolysis, Fig. 6 shows the variation of concentrations of all identified chlorine species (Cl^- , HClO/ClO^- , ClO_3^- , ClO_4^-) with electrooxidation time at 1.45 and 43.5 mA cm^{-2} . The formation of hypochlorite species (HClO and ClO^-) occurred during electrolysis at both current densities and related to the electric charge (Fig. 6 (c)).

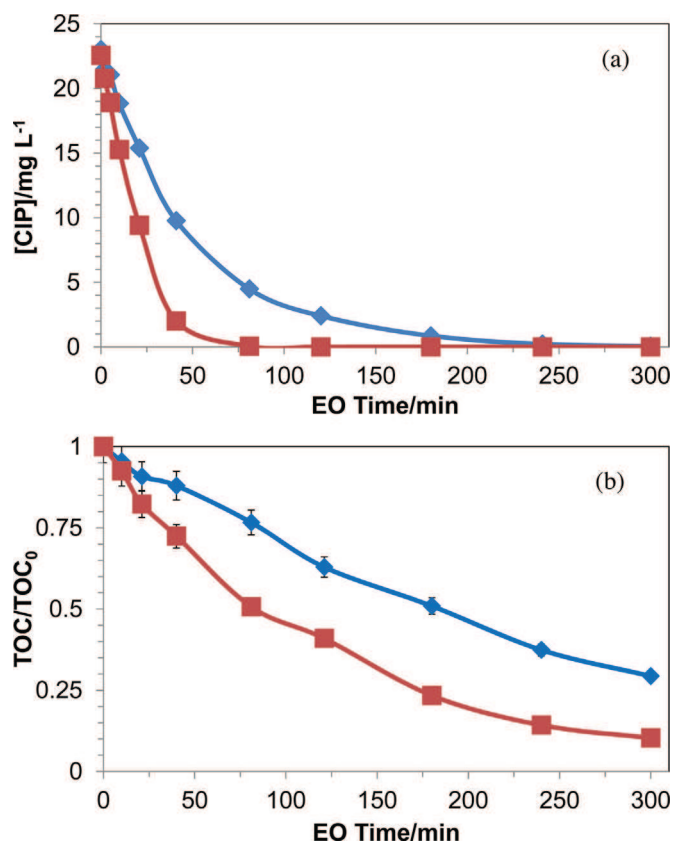


Fig. 5. Variation of CIP (a) and TOC (b) in \blacklozenge K_2SO_4 0.02 mol L^{-1} , \blacksquare K_2SO_4 $0.02 \text{ mol L}^{-1} + 2.25 \text{ mmol L}^{-1} \text{ KCl}$, during electrolysis of 1L CIP solution, $[\text{CIP}]_0 = 22.30 \text{ mg L}^{-1}$ ($0.068 \text{ mmol L}^{-1}$), $[\text{TOC}]_0 = 12 \text{ mg L}^{-1}$, $i = 1.45 \text{ mA cm}^{-2}$ ($i^0_{\text{lim}} = 1.29 \text{ mA cm}^{-2}$), initial pH=6.

When the current density was close to the limiting current density ($i = 1.45 \text{ mA cm}^{-2}$), Cl^- was oxidized in hypochlorite and no other species was observed (the sum of the concentration of Cl^- and ClO^- equaled the initial concentration of Cl^-). At higher current intensities (43.5 mA cm^{-2}), ClO^- and ClO_4^- were formed at the beginning of electrolysis. The concentration of ClO^- reached a maximum value of 0.42 mM at 20 min, then decreased to 0.05 mM at 120 min and disappeared at the end of electrolysis. The concentration of ClO_3^- during electrolysis at 43.5 mA cm^{-2} was lower than the quantification limit of ionic chromatography ($< 1 \text{ ppm}$). After 300 min of electrolysis, 90% of chloride was converted into perchlorate, which was the major chlorine species in the solution at 43.5 mA cm^{-2} .

It is evidenced that the formation of ClO_4^- is highly related to the applied current density, rather than the electric charge. Since, for an electrical charge of 0.5 Ah L^{-1} , a quarter of Cl^- was removed and half of it was converted into perchlorate at a high current density (43.47 mA cm^{-2}); at 1.45 mA cm^{-2} , all the disappeared Cl^- were in the form of ClO^- . This phenomenon can be attributed to the fact that more oxygen species (mainly $\bullet\text{OH}$) are electrogenerated for high applied current densities. It is known that electrogenerated oxygen species play an important role in the generation of ClO_4^- from Cl^- [36,37,60] (see equation 6 and table). Azizi et al. have shown that on the BDD anode, the HClO_4 is formed by the homogeneous reaction between ClO_3^* and $\bullet\text{OH}$ [39]. The high concentration of electrogenerated oxygen species allows the reactions between the intermediate chlorine species and oxygen species to form ClO_4^- . This explanation is also supported by the studies of Jung et al. [36] showing that the electrogeneration rate of ClO_4^- depended on the concentration of oxygen species ($\bullet\text{OH}$,

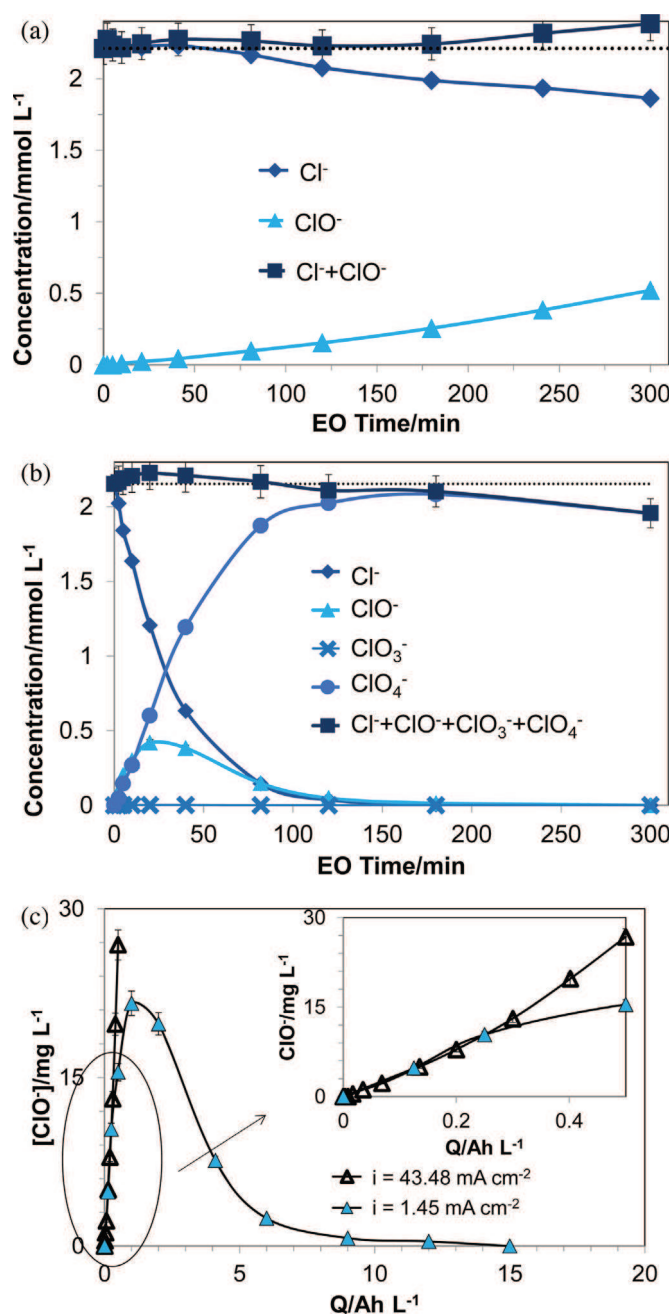


Fig. 6. Concentration of chlorine species during electrolysis of K_2SO_4 0.02 mol L^{-1} and 2.25 mmol L^{-1} KCl solution containing CIP: Cl^- (\blacklozenge); $Cl^- + ClO^- + ClO_4^-$ (\blacksquare); (b) ClO^- (\blacktriangle), ClO_3^- (\times) ClO_4^- (\bullet) (a) $i = 1.45 \text{ mA cm}^{-2}$, (b) $i = 43.48 \text{ mA cm}^{-2}$, (3) ClO^- versus the electrical charge, initial pH=6. The dashed line is the total concentration of chlorine compounds in the solution. Error bars = $\pm 1.5\%$ for Cl^- , $\pm 2\%$ for ClO_4^- , $\pm 5\%$ for ClO^- .

Table 5
Concentration of AOX at initial time and after 300 min of electrolysis. Operating conditions: Fig. 6.

$[Cl^-]_0$ (mg L^{-1})	Current density (mA cm^{-2})	EO time (min)	Q (Ah L^{-1})	TOC (mg L^{-1})	AOX ($\mu\text{g L}^{-1} \text{ Cl}$)
78.0	0	0	0	12	< LD
78.5	1.45	300	0.5	1.1	370
76.5	43.5	300	15	6.8	4600

H_2O_2 , O_3). A faster generation rate of ClO_4^- was observed for higher concentrations of oxygen species.

Moreover, the presence of organics, such as CIP which are scavengers of $\cdot OH$ may significantly limit the production of perchlorate. The obvious decrease in chloride concentrations only occurred after approximately 40 min of electrolysis, when 90% of CIP was removed at 1.45 mA cm^{-1} . Conversely, higher current densities (43.47 mA cm^{-1}), chloride is oxidized from the beginning of the electrolysis.

It is interesting to find that intermediate species, such as ClO_2^- and ClO_3^- were not observed before the formation of ClO_4^- at 43.5 mA cm^{-1} . This is probably due to the electrochemical BDD anode's properties and the high applied current density. Radical sites (for example $C-O\cdot$ and $C\cdot$) on the BDD anode surface act as adsorption sites for $ClO_x\cdot$ radicals on anode surfaces [32]. Radical sites can stabilize the $ClO_x\cdot$ radicals and increase their life time, leading to favor their reaction with electrogenerated oxygen species (mainly $\cdot OH$) in the area close to the anode. The relatively large concentration of hydroxyl radicals for a high current density make it possible to directly form the terminal product (ClO_4^-).

Furthermore, it can be observed from Fig. 6 (b) that the final concentration of the chlorine species (ClO_4^-) was lower than the initial concentration of Cl^- . The risk of forming AOXs which are toxic to the environment and human health, seems to exist, in particular for high current intensities. Table 5 highlights that for a current density of 43.5 mA cm^{-2} , the quantity of AOXs at the end of electrolysis is 13 times higher than that for a current density of 1.45 mA cm^{-2} .

Addition and substitution reactions between organic compounds and active chlorine (e.g., Cl_2 , OCl , $HOCl$) or chlorine radicals ($Cl\cdot$, $ClO_x\cdot$) are the principal reasons for the formation of AOXs [32]. At high current density (43.5 mA cm^{-2}) the amount of these electrogenerated chlorine species is very high. In particular the chlorine radicals, which can be formed on the electrode surface (equation b, e, g, Table 1) and also possibly in the bulk with the electrogenerated oxygen species (e.g. $\cdot OH$, H_2O_2). For example, in the bulk, ClO^- reacts with electrogenerated H_2O_2 to form a hypochlorite radical as Eq. 14 and 15 [61,62].



Consequently, using a high current density ($\frac{i}{i_{lim}} > 30$) in such electrochemical processes poses the risks of the formation of AOXs. Furthermore, the significant formation of AOX at 43.5 mA cm^{-2} explains the low removal of TOC (40%) at the end of electrolysis. This TOC is likely to be rather refractory to the electrooxidation: the value is stable from 120 mins' (6 Ah L^{-1}) to 300 min (15 Ah L^{-1}) electrolysis.

Thus, the choice of the appropriate current density ($i \approx i_{lim}^0$) is important to limit the formation of refractory and toxic compounds such as ClO_4^- and AOXs for the application of electrochemical oxidation with the BDD to treat wastewater in the presence of chloride.

3.4. Electrochemical oxidation treatment of real wastewater

3.4.1. Effect of matrix on the removal of target pharmaceuticals and COD

Electrolysis was carried out with NF retentate of biologically-treated hospital wastewater. The physico-chemical characteristics and composition of the wastewater are presented in Table 3. Fig. 7 shows the variation of concentrations of CIP and COD in wastewater during electrolysis.

The CIP was totally removed after 80 min (0.4 Ah L^{-1}). It can be observed that during the first 15 minutes CIP degraded fast in a higher rate, thereafter the degradation rate decreased. The change in the degradation rate was possibly induced by the production of several kinds of intermediates. These may compete with CIP for oxidation and slow down the observed CIP degradation rate in the complex matrix. Nonetheless, the degradation rate of CIP in the NF retentate matrix (0.091 min^{-1} for the first 15 min and then 0.034 min^{-1}) was higher than the one obtained in the synthetic solution (performed under the same applied current density): 0.028 min^{-1} . It can be suggested that some additional phenomena occurred during the electrochemical oxidation of wastewater. As discussed in section 3.2, the oxidants electrogenerated from salts, such as $\text{SO}_4^{\bullet-}$ and hypochlorite can accelerate the degradation of CIP. The similar faster removal of COD was observed after 120 min of electrolysis (Fig. 7 (b)). The calculation of faradic efficiency (ICE) as function of COD values shows that ICE decreases from 44% to 10% between 10 and 180 minutes of electrolysis. At the beginning of electrolysis, the decay of COD was in excellent accordance with theoretical values. After 120 min the difference between the

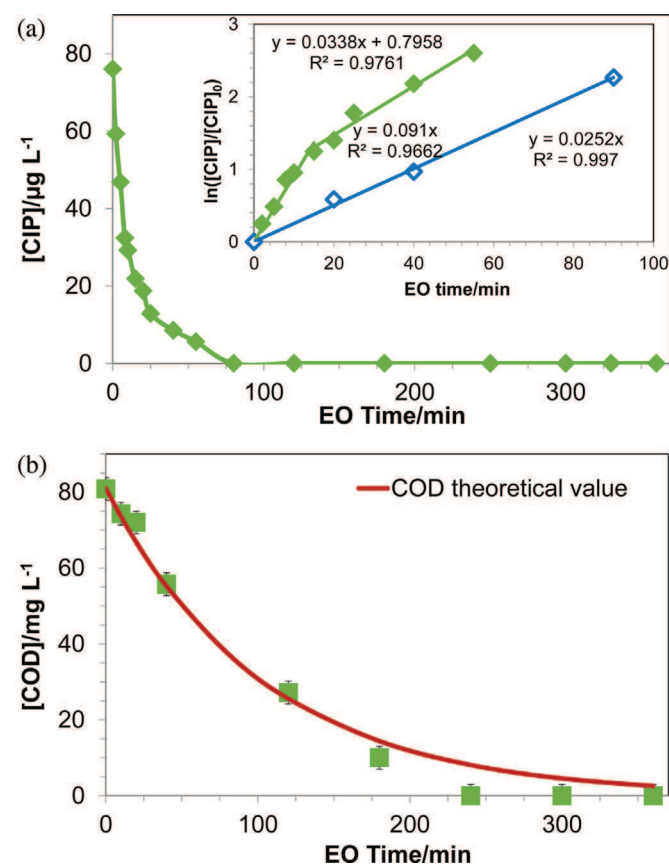


Fig. 7. Removal of CIP (a) and COD (b) with electrochemical oxidation time during 360 mins' of electrolysis of 1L NF retentate. $[\text{CIP}]_0 = 76 \mu\text{g L}^{-1}$ ($0.023 \text{ mmol L}^{-1}$), $\text{COD}_0 = 81 \text{ mg L}^{-1}$, $i = 4.34 \text{ mA cm}^{-2}$ ($i_{\text{lim}}^0 = 2.25 \text{ mA cm}^{-2}$), $\text{pH} = 8$. Inset panel: kinetic analysis of pharmaceuticals during EO under mass transfer control in NF retentate (full symbols) and in synthetic solution (empty symbols).

experimental and the theoretical values can be explained by the effect of the reaction with the electrogenerated oxidants from salts.

3.4.2. Conversion of ions (in particular Cl^-) during electrolysis

The presence of Cl^- in the process must be studied carefully, particularly to the possible formation of toxic by-products. Fig. 8 presents the conversion of chlorine species during 360 min electrolysis of 1L NF retentate. It appears that the concentration of Cl^- declined with time and that ClO^- and ClO_4^- were formed (concentration of ClO_3^- was lower than the quantification limits, that are $< 1 \text{ mg L}^{-1}$). This electrolysis was performed with a real wastewater which contains many organics including halogenated organics. Thus, the initial quantity of chlorinated species is unknown. During the electrolysis, the oxidation of such compounds may produce chloride ions or perchlorate. Consequently, a complete mass balance of chlorinated species cannot be achieved.

When the applied current density was close to the limiting current ($i = 4.34 \text{ mA cm}^{-2}$, $i_{\text{lim}}^0 = 2.25 \text{ mA cm}^{-2}$), the generation of undesired perchlorate ClO_4^- has been observed only after 180 min. At this time, the target pharmaceutical (e.g. CIP) was completely degraded and 86% of COD was removed. The ClO_4^- appeared only after 120 minutes and reached 3 mg L^{-1} at the end of electrolysis. As though that the presence of organics in the NF retentate inhibited the formation of ClO_4^- at the beginning of electrolysis, then the inhibition effect weakened with the decrease in organic concentration. This explanation is in accordance with the study of Donaghue and Chaplin [43] in which the organics acted as $\bullet\text{OH}$ scavengers and compete with ClO_3^{\bullet} , which was the intermediate of ClO_4^- formation. In other words, based on Eq. 8, the limiting current density decreases with COD decay. Herein, at 180 min ($\frac{i}{i_{\text{lim}}(180)} > 26$), as discussed in section 3.3.2, the use of high current density favors the formation of ClO_4^- . Consequently, the applied current density, but also the electrooxidation time are very significant for limiting of the ClO_4^- formation. Another possible strategy would be to adjust the value of the applied current density with the COD value, according to Eq. 8.

In addition, it is worth noting that 80% of AOXs present in the NF retentate (initial AOX = $2300 \mu\text{g Cl L}^{-1}$ and final AOX = $450 \mu\text{g Cl L}^{-1}$) were removed after 360 min of electrolysis.

Regarding the other mineral salts, (figure is given in Supplementary Materials S1), on one hand, the concentration of NO_3^- and SO_4^{2-} increased slightly during the process and stabilized which can be explained by the degradation of organics containing atoms of S and N. On the other hand, one can observe a significant decrease in the concentrations of Mg^{2+} , PO_4^{3-} , Ca^{2+} and HCO_3^- . This decrease can be attributed to the scaling, which occurred on the

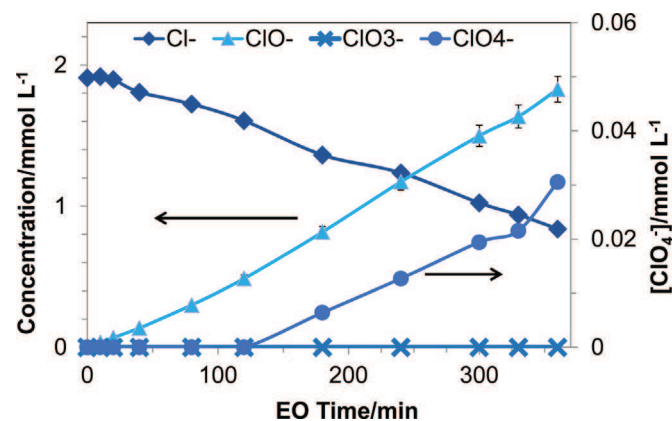


Fig. 8. Variation of concentrations of chlorine species during 360 mins' electrolysis of 1L NF retentate: Cl^- (\blacklozenge); (b) ClO^- (\blacktriangle), ClO_3^- (\square) ClO_4^- (\bullet), $\text{pH} = 7.8$, $[\text{Cl}^-]_0 = 2 \text{ mmol L}^{-1}$, operating conditions: see Fig. 7.

electrolysis cell. Indeed, during electrolysis, the electrochemical reduction of dissolved oxygen and water leads to the increase of the local pH. The generation of hydroxyl ions disturbs the calcium-carbonic equilibrium of the solution. Hydrocarbonate ions (HCO_3^-) are converted into carbonate ions (Eq. 16):



Carbonate ions may react with calcium ions to form calcium carbonate on the cathode surface.



In the same way, the precipitation of $\text{Mg}(\text{OH})_2$ happens at the cathodes [63].



To verify this hypothesis, the electrochemical cell was washed with pure water and then rinsed with 0.7 L of H_2SO_4 0.1 M solution for one hour. The acidic solution was analyzed before and after washing. The rate of recovery for Mg^{2+} , PO_4^{3-} , Ca^{2+} after acidified rinse was relatively satisfactory, with an accuracy of 20%. Even if scaling occurred during electrolysis, the increase in cell potential was not observed during electrolysis. The deposit of scaling should be porous and should not hinder the electron transfer. However, the long-term effect should be shortening the service life of the electrodes. The satisfactory rate of recovery of Mg^{2+} , PO_4^{3-} , Ca^{2+} indicates that a simple rinse with acidic solution can be an effective method to deal with the scaling of the cell. Regular recirculation with an acidic solution in the electrolysis system could be an efficient strategy for protecting the electrode. Another treatment consists of regularly applying reversal of electrode polarity, in order to limit electrochemically dissolve the deposition of scale.

4. Conclusion

Beyond the increase in conductivity of the solution, the presence of salts in the solution generally induces an increase in the removal rate of pharmaceuticals, the chemical oxygen demand and total organic carbon. Strong oxidants can be electrogenerated from salts during electrochemical oxidation; these oxidants enable to react chemically with organics. This is particularly true for chloride and sulfate anions. The latter in contact with hydroxyl radicals form sulfate radicals that react selectively with organic compounds: the presence of sulfates accelerated the removal of CIP and SMX, but had no effect on the oxidation of SALBU. A remarkable acceleration of CIP degradation was also observed in presence of Cl^- . However, electrooxidation at high current densities surprisingly had adverse effect on the mineralization of pharmaceuticals. TOC removal indicated in presence of Cl^- at $i \approx i_{\text{lim}}^0$ from 70% to 90%, while dramatically decreased to 40% when $\frac{i}{i_{\text{lim}}} > 30$. The significantly quantity of AOXs formed at higher current densities can explain the low removal rate of TOC. The formation of other undesired by-products: ClO_4^- was only observed at high current densities ($\frac{i}{i_{\text{lim}}} > 30$). The formation of ClO_4^- and AOXs is strongly related to the applied current density rather than the electric charge. This can be explained by the fact that, under these operating conditions, many hydroxyl radicals are produced and consequently, many oxygen atoms are transferred to the chlorine species and organics to form perchlorate and AOXs. This tendency has been confirmed during electrolysis of real wastewaters. Perchlorate appeared when the organic matter has nearly completely degraded.

These results highlight that it is very important to control the electrolysis time in order to limit perchlorate formation or to adapt

the value of the applied current density with the COD value according to the theoretical model of COD decay.

Moreover, the presence of Ca^{2+} , Mg^{2+} and inorganic carbon entails scaling which is due to the increase of the local pH at the cathode. A regular rinsing of the electrochemical cell with acidic solution or an electrochemical treatment consisting in reversal polarity can be proposed to limit the decrease of lifetime of electrode. The cleaning frequency should be adjusted according to the hardness of the solution.

Acknowledgment

The authors would like to thank the China scholarship council for the final support. They are also grateful to the coordinator of the PANACEE project supported by the French National Research Agency for allowing us access to hospital wastewater. They would like to thank the Laboratoire Départemental 31: Eau-Vétérinaire-Air in Toulouse for the analysis of AOXs. Lastly, they would also like to thank Sophie Chambers for proof reading and correcting the manuscript.

Appendix A. Supplementary data

Supplementary material related to this article can be found, in the online version, at <http://dx.doi.org/10.1016/j.electacta.2017.01.160>.

References

- [1] E. Zuccato, D. Calamari, M. Natangelo, R. Fanelli, Presence of therapeutic drugs in the environment, *The Lancet*. 355 (2000) 1789–1790.
- [2] D.W. Kolpin, E.T. Furlong, M.T. Meyer, E.M. Thurman, S.D. Zaugg, L.B. Barber, H. T. Buxton, Pharmaceuticals, Hormones, and Other Organic Wastewater Contaminants in U.S. Streams, 1999 – 2000: A National Reconnaissance, *Environ. Sci. Technol.* 36 (2002) 1202–1211.
- [3] X. Chang, M.T. Meyer, X. Liu, Q. Zhao, H. Chen, J. Chen, Z. Qiu, L. Yang, J. Cao, W. Shu, Determination of antibiotics in sewage from hospitals, nursery and slaughter house, wastewater treatment plant and source water in Chongqing region of Three Gorge Reservoir in China, *Environ. Pollut.* 158 (2010) 1444–1450.
- [4] K.S. Le Corre, C. Ort, D. Kateley, B. Allen, B.I. Escher, J. Keller, Consumption-based approach for assessing the contribution of hospitals towards the load of pharmaceutical residues in municipal wastewater, *Environ. Int.* 45 (2012) 99–111.
- [5] K. Kümmerer, Significance of antibiotics in the environment, *J. Antimicrob. Chemother.* 52 (2003) 5–7.
- [6] G.M. Bruce, R.C. Pleus, S.A. Snyder, Toxicological Relevance of Pharmaceuticals in Drinking Water, *Environ. Sci. Technol.* 44 (2010) 5619–5626.
- [7] A.J. Watkinson, E.J. Murby, D.W. Kolpin, S.D. Costanzo, The occurrence of antibiotics in an urban watershed: From wastewater to drinking water, *Sci. Total Environ.* 407 (2009) 2711–2723.
- [8] M. Clara, N. Kreuzinger, B. Strenn, O. Gans, H. Kroiss, The solids retention time—a suitable design parameter to evaluate the capacity of wastewater treatment plants to remove micropollutants, *Water Res.* 39 (2005) 97–106.
- [9] S. Rodriguez-Mozaz, S. Chamorro, E. Marti, B. Huerta, M. Gros, A. Sánchez-Melsió, C.M. Borrego, D. Barceló, J.L. Balcázar, Occurrence of antibiotics and antibiotic resistance genes in hospital and urban wastewaters and their impact on the receiving river, *Water Res.* 69 (2015) 234–242.
- [10] L. Kovalova, H. Siegrist, H. Singer, A. Wittmer, C.S. McArdell, Hospital Wastewater Treatment by Membrane Bioreactor: Performance and Efficiency for Organic Micropollutant Elimination, *Environ. Sci. Technol.* 46 (2012) 1536–1545.
- [11] I. Sires, E. Brillas, Remediation of water pollution caused by pharmaceutical residues based on electrochemical separation and degradation technologies: A review, *Environ. Int.* 40 (2012) 212–229.
- [12] R. Tenne, K. Patel, K. Hashimoto, A. Fujishima, An International Journal Devoted to all Aspects of Electrode Kinetics, Interfacial Structure, Properties of Electrolytes, Colloid and Biological Electrochemistry Efficient electrochemical reduction of nitrate to ammonia using conductive diamond film electrodes, *J. Electroanal. Chem.* 347 (1993) 409–415.
- [13] M. Murugananthan, S. Yoshihara, T. Rakuma, N. Uehara, T. Shirakashi, Electrochemical degradation of 17 β -estradiol (E2) at boron-doped diamond (Si/BDD) thin film electrode, *Electrochimica Acta.* 52 (2007) 3242–3249.
- [14] R.F. Brocenschi, R.C. Rocha-Filho, N. Bocchi, S.R. Biaggio, Electrochemical degradation of estrone using a boron-doped diamond anode in a filter-press reactor, *Electrochimica Acta.* 197 (2016) 186–193.

- [15] E. Brillas, I. Sirés, C. Arias, P.L. Cabot, F. Centellas, R.M. Rodríguez, J.A. Garrido, Mineralization of paracetamol in aqueous medium by anodic oxidation with a boron-doped diamond electrode, *Chemosphere*. 58 (2005) 399–406.
- [16] J. Boudreau, D. Bejan, S. Li, N.J. Bunce, Competition between Electrochemical Advanced Oxidation and Electrochemical Hypochlorination of Sulfamethoxazole at a Boron-Doped Diamond Anode, *Ind. Eng. Chem. Res.* 49 (2010) 2537–2542.
- [17] K.P. de Amorim, L.L. Romualdo, L.S. Andrade, Electrochemical degradation of sulfamethoxazole and trimethoprim at boron-doped diamond electrode: Performance, kinetics and reaction pathway, *Sep. Purif. Technol.* 120 (2013) 319–327.
- [18] M. Murugananthan, S.S. Latha, G. Bhaskar Raju, S. Yoshihara, Role of electrolyte on anodic mineralization of atenolol at boron doped diamond and Pt electrodes, *Sep. Purif. Technol.* 79 (2011) 56–62.
- [19] G. Perez, A.R. Fernandez-Alba, A.M. Urriaga, I. Ortiz, Electro-oxidation of reverse osmosis concentrates generated in tertiary water treatment, *Water Res.* 44 (2010) 2763–2772.
- [20] A.M. Urriaga, G. Pérez, R. Ibáñez, I. Ortiz, Removal of pharmaceuticals from a WWTP secondary effluent by ultrafiltration/reverse osmosis followed by electrochemical oxidation of the RO concentrate, *Desalination*. 331 (2013) 26–34.
- [21] Y. Lan, C. Coetsier, C. Causserand, K.G. Serrano, Feasibility of Micropollutants Treatment by Coupling Nanofiltration and Electrochemical Oxidation: Case of Hospital Wastewater, *Int. J. Chem. React. Eng.* 13 (2015) 153–159.
- [22] K. Groenen-Serrano, Wastewater Treatment by Electrogeneration of Strong Oxidants Using Borondoped Diamond (BDD), in: G. Kreysa, K. Ota, R.F. Savinell (Eds.), *Encycl. Appl. Electrochem.*, Springer, New York, 2014, pp. 2126–2132.
- [23] K. Serrano, P.A. Michaud, C. Comninellis, A. Savall, Electrochemical preparation of peroxodisulfuric acid using boron doped diamond thin film electrodes, *Electrochimica Acta*. 48 (2002) 431–436.
- [24] I.M. Kolthoff, I.K. Miller, The Chemistry of Persulfate. I. The Kinetics and Mechanism of the Decomposition of the Persulfate Ion in Aqueous Medium, *J. Am. Chem. Soc.* 73 (1951) 3055–3059.
- [25] M. Murugananthan, S.S. Latha, G. Bhaskar Raju, S. Yoshihara, Anodic oxidation of ketoprofen—An anti-inflammatory drug using boron doped diamond and platinum electrodes, *J. Hazard. Mater.* 180 (2010) 753–758.
- [26] M.E.H. Bergmann, J. Rollin, T. Iourtchouk, The occurrence of perchlorate during drinking water electrolysis using BDD anodes, *Electrochimica Acta*. 54 (2009) 2102–2107.
- [27] C.R. Costa, F. Montilla, E. Morallón, P. Olivi, Electrochemical oxidation of acid black 210 dye on the boron-doped diamond electrode in the presence of phosphate ions: Effect of current density, pH, and chloride ions, *Electrochimica Acta*. 54 (2009) 7048–7055.
- [28] V. Schmalz, T. Dittmar, D. Haaken, E. Worch, Electrochemical disinfection of biologically treated wastewater from small treatment systems by using boron-doped diamond (BDD) electrodes – Contribution for direct reuse of domestic wastewater, *Water Res.* 43 (2009) 5260–5266.
- [29] O. Scialdone, S. Randazzo, A. Galia, G. Silvestri, Electrochemical oxidation of organics in water: Role of operative parameters in the absence and in the presence of NaCl, *Water Res.* 43 (2009) 2260–2272.
- [30] Á. Anglada, A. Urriaga, I. Ortiz, D. Mantzavinos, E. Diamadopoulos, Boron-doped diamond anodic treatment of landfill leachate: Evaluation of operating variables and formation of oxidation by-products, *Water Res.* 45 (2011) 828–838.
- [31] E.T. Urbansky, M.R. Schock, Issues in managing the risks associated with perchlorate in drinking water, *J. Environ. Manage.* 56 (1999) 79–95.
- [32] B.P. Chaplin, Critical review of electrochemical advanced oxidation processes for water treatment applications, *Environ. Sci. Process. Impacts*. 16 (2014) 1182–1203.
- [33] K. Viswanathan, B.V. Tilak, Chemical, Electrochemical, and Technological Aspects of Sodium Chlorate Manufacture, *J. Electrochem. Soc.* 131 (1984) 1551–1559.
- [34] M.S. Siddiqui, Chlorine-ozone interactions: Formation of chlorate, *Water Res.* 30 (1996) 2160–2170.
- [35] L.R. Czarnetzki, L.J.J. Janssen, Formation of hypochlorite, chlorate and oxygen during NaCl electrolysis from alkaline solutions at an RuO₂/TiO₂ anode, *J. Appl. Electrochem.* 22 (1992) 315–324.
- [36] Y.J. Jung, K.W. Baek, B.S. Oh, J.-W. Kang, An investigation of the formation of chlorate and perchlorate during electrolysis using Pt/Ti electrodes: The effects of pH and reactive oxygen species and the results of kinetic studies, *Water Res.* 44 (2010) 5345–5355.
- [37] A.M. Polcaro, A. Vacca, M. Mascia, S. Palmas, J.R. Ruiz, Electrochemical treatment of waters with BDD anodes: kinetics of the reactions involving chlorides, *J. Appl. Electrochem.* 39 (2009) 2083–2092.
- [38] M.E.H. Bergmann, J. Rollin, Product and by-product formation in laboratory studies on disinfection electrolysis of water using boron-doped diamond anodes, *Catal. Today*. 124 (2007) 198–203.
- [39] O. Azizi, D. Hubler, G. Schrader, J. Farrell, B.P. Chaplin, Mechanism of Perchlorate Formation on Boron-Doped Diamond Film Anodes, *Environ. Sci. Technol.* 45 (2011) 10582–10590.
- [40] C. do, N. Brito, D.M. de Araújo, C.A. Martínez-Huitle, M.A. Rodrigo, Understanding active chlorine species production using boron doped diamond films with lower and higher sp³/sp² ratio, *Electrochem. Commun.* 55 (2015) 34–38.
- [41] S. Ferro, A.D. Battisti, I. Duo, C. Comninellis, W. Haenni, A. Perret, Chlorine Evolution at Highly Boron-Doped Diamond Electrodes, *J. Electrochem. Soc.* 147 (2000) 2614–2619, doi:http://dx.doi.org/10.1149/1.1393578.
- [42] Y. Yang, J.J. Pignatello, J. Ma, W.A. Mitch, Comparison of Halide Impacts on the Efficiency of Contaminant Degradation by Sulfate and Hydroxyl Radical-Based Advanced Oxidation Processes (AOPs), *Environ. Sci. Technol.* 48 (2014) 2344–2351, doi:http://dx.doi.org/10.1021/es404118q.
- [43] A. Donaghue, B.P. Chaplin, Effect of Select Organic Compounds on Perchlorate Formation at Boron-doped Diamond Film Anodes, *Environ. Sci. Technol.* 47 (2013) 12391–12399, doi:http://dx.doi.org/10.1021/es4031672.
- [44] I. Quesada, Y. Gonzalez, S. Schetrite, H. Budzinski, K. Le Menach, O. Lorain, N. Manier, S. Ait Aissa, P. Pandard, D. Abdelaziz, J.-M. Canonge, C. Albasi, PANACÉE: évaluation du fonctionnement d'un bioréacteur à membranes immergées traitant des effluents hospitaliers d'oncologie, *Rev. Sci. Eau*. 28 (2015) 1.
- [45] ISO 9562:2004(en) Water quality – Determination of adsorbable organically bound halogens (AOX)
- [46] C. Racaud, A. Savall, P. Rondet, N. Bertrand, K. Groenen Serrano, New electrodes for silver(II) electrogeneration: Comparison between Ti/Pt, Nb/Pt, and Nb/BDD, *Chem. Eng. J.* 211–212 (2012) 53–59.
- [47] M. Panizza, P.A. Michaud, G. Cerisola, C. Comninellis, Anodic oxidation of 2-naphthol at boron-doped diamond electrodes, *J. Electroanal. Chem.* 507 (2001) 206–214.
- [48] C. Sonntag, U. von Gunten, *Chemistry of Ozone in Water and Wastewater Treatment: From Basic Principles to Applications*, IWA Publishing, 2012.
- [49] H. Lutze, Sulfate radical based oxidation in water treatment, *Universität Duisburg-Essen*, 2013.
- [50] Ionization Constants of Inorganic Monoprotic Acids, [Chemistry.msu.edu](http://chemistry.msu.edu).
- [51] P. Neta, V. Madhavan, H. Zemel, R.W. Fessenden, Rate constants and mechanism of reaction of sulfate radical anion with aromatic compounds, *J. Am. Chem. Soc.* 99 (1977) 163–164.
- [52] I.T. Osgerby, ISCO Technology Overview: Do You Really Understand the Chemistry? in: E.J. Calabrese, P.T. Kostecki, J. Dragun (Eds.), *Contam. Soils Sediments Water*, Springer-Verlag, 2006, pp. 287–308.
- [53] Y. Ji, C. Ferronato, A. Salvador, X. Yang, J.-M. Chovelon, Degradation of ciprofloxacin and sulfamethoxazole by ferrous-activated persulfate: Implications for remediation of groundwater contaminated by antibiotics, *Sci. Total Environ.* 472 (2014) 800–808.
- [54] M.M. Ahmed, S. Barbati, P. Doumenq, S. Chiron, Sulfate radical anion oxidation of diclofenac and sulfamethoxazole for water decontamination, *Chem. Eng. J.* 197 (2012) 440–447.
- [55] C. Liang, Z.-S. Wang, C.J. Bruell, Influence of pH on persulfate oxidation of TCE at ambient temperatures, *Chemosphere*. 66 (2007) 106–113.
- [56] F. Minisci, A. Citterio, C. Giordano, Electron-transfer processes: peroxydisulfate, a useful and versatile reagent in organic chemistry, *Acc. Chem. Res.* 16 (1983) 27–32.
- [57] G.R.P. Malpass, D.W. Miwa, S.A.S. Machado, P. Olivi, A.J. Motheo, Oxidation of the pesticide atrazine at DSA® electrodes, *J. Hazard. Mater.* 137 (2006) 565–572.
- [58] M. Panizza, G. Cerisola, Application of diamond electrodes to electrochemical processes, *Electrochimica Acta*. 51 (2005) 191–199.
- [59] T.N. Das, Reactivity and Role of SO₅•- Radical in Aqueous Medium Chain Oxidation of Sulfite to Sulfate and Atmospheric Sulfuric Acid Generation, *J. Phys. Chem. A*. 105 (2001) 9142–9155.
- [60] H. Li, J. Ni, Electrogeneration of disinfection byproducts at a boron-doped diamond anode with resorcinol as a model substance, *Electrochimica Acta*. 69 (2012) 268–274.
- [61] C. Flox, E. Brillas, A. Savall, K. Groenen-Serrano, Kinetic Study of the Electrochemical Mineralization of m-Cresol on a Boron-Doped Diamond Anode, *Curr. Org. Chem.* 16 (2012) 1960–1966.
- [62] R. Castagna, J.P. Eiserich, M.S. Budamagunta, P. Stipa, C.E. Cross, E. Proietti, J.C. Voss, L. Greci, Hydroxyl radical from the reaction between hypochlorite and hydrogen peroxide, *Atmos. Environ.* 42 (2008) 6551–6554.
- [63] A. Kraft, M. Stadelmann, M. Blaschke, D. Kreysig, B. Sandt, F. Schröder, J. Rennau, Electrochemical water disinfection Part I: Hypochlorite production from very dilute chloride solutions, *J. Appl. Electrochem.* 29 (1999) 859–866.